Geoderma 281 (2016) 39–48

Contents lists available at ScienceDirect

Geoderma

journal homepage: www.elsevier.com/locate/geoderma

The effects of rock fragment shapes and positions on modeled hydraulic conductivities of stony soils

Hana Hlaváčiková [a,*], Viliam Novák [a], Jirka Šimůnek [b]

[a] Institute of Hydrology, Slovak Academy of Sciences, Dúbravská cesta 9, 84104 Bratislava, Slovakia
[b] Dept. of Environmental Sciences, Univ. of California Riverside, Riverside, CA 92521, USA

ARTICLE INFO

Article history:
Received 21 December 2015
Received in revised form 6 June 2016
Accepted 27 June 2016
Available online xxxx

Keywords:
Soil matrix
Rock fragments
Effective saturated hydraulic conductivity
HYDRUS-2D modeling

ABSTRACT

Mountainous soils usually contain a large number of rock fragments, particles with a diameter larger than 2 mm, which can influence soil hydraulic properties that are required to quantitatively describe soil water movement in stony soils. The objective of this study was to numerically estimate both the saturated hydraulic conductivity of a stony soil and its dependence on a relative content of rock fragments (stoniness), and the shape, position and distribution of rock fragments in a soil matrix. The assessment method was based on a numerical version of Darcy's classic experiment that involved steady-state flow through a porous material under a unit hydraulic gradient. Our experiments, involving hypothetical stony soils in this particular case, were simulated using mainly the two-dimensional (2D) numerical model, HYDRUS-2D. A limited number of simulations were carried out using a three-dimensional HYDRUS model. Three different shapes of hypothetical rock fragments were used in the study: a sphere, an ellipsoid with two different positions, and a pyramid, all represented by their 2D cross-sections (i.e., a circle, an ellipse, and a triangle, respectively). The mean relative effective saturated hydraulic conductivity (K_{rs}) for the same stoniness was almost the same for all simulated scenarios and fine soil textures. A stoniness between 0.07 and 0.5 $cm^3\ cm^{-3}$ can cause a decrease of K_{rs} in the range of 0.17–0.70. Numerical experiments were divided into 3 scenarios. The largest and the smallest values of K_{rs} were different for different shapes of RFs (scenario A), different orientations of the slab-sided elliptical RFs (scenario B), and regular or irregular distributions of spherical RFs (scenario C). The largest difference between K_{rs} values (0.26) was found in scenario B when the slab-sided elliptical RFs were oriented either horizontally or vertically for stoniness of 0.24 or 0.31 cm^3cm^{-3}. Simulated K_{rs} values were underestimated in all scenarios as compared to the Ravina and Magier (1984) function. The smallest differences (−1.1%–2.5%) between numerically simulated and calculated (the Corring and Churchill (1961) method for a cylindrical shape of RFs) K_{rs} values were found for scenario A with its 2D representation of spherical rock fragments. Calculated (the Corring and Churchill (1961) method for a spherical shape of RFs) K_{rs} values corresponded well with those simulated using a 3D representation of spherical rock fragments. Numerical models provide a unique opportunity to evaluate the effects of different factors on the saturated hydraulic conductivity of stony soils that may be nearly impossible to measure in practice.

1. Introduction

Soils containing a significant fraction of rock fragments (RF) are generally denoted as stony soils and can be present in many forested and mountainous areas. The shape, size, degree of weathering, and geological origin of rock fragments can all strongly influence the soil's hydrophysical properties, especially the soil's water retention and hydraulic conductivity (Brouwer and Anderson, 2000; Cousin et al., 2003). According to Poesen and Lavee (1994), about 30% of soils in Western Europe and about 60% of soils in the Mediterranean region are stony soils. According to Šály (1978), up to 80% of Slovak forest soils contain stones and their stone content generally increases with depth. Furthermore, about 47% of Slovak agricultural soils are referred to as stony soils (Hraško and Bedrna, 1988). The spatial distribution of rock fragment in hillslopes is mostly controlled by slope gradient and topographic position (Chen et al., 2012). It is expected that rock fragments, and their size, shape, position, and spatial distribution in the soil, can strongly influence the stony soils' properties and can affect

Abbreviations: RF, rock fragments; REV, representative elementary volume; RM, the Ravina and Magier (1984) function; CCS, the Corring and Churchill (1961) function for a spherical shape of rock fragments; CCC, the Corring and Churchill (1961) function for a cylindrical shape of rock fragments.

* Corresponding author.
E-mail address: hlavacikova@uh.savba.sk (H. Hlaváčiková).

http://dx.doi.org/10.1016/j.geoderma.2016.06.034
0016-7061/

soil water movement, infiltration (Al-Qinna et al., 2014; Chen et al., 2012), and the occurrence of runoff (Hlaváčiková et al., 2015).

Stony soils are composed of a soil matrix, small particles with a diameter of less than 2 mm, and larger rock fragments, e.g., gravel, cobbles, stones, and boulders. The most important characteristics of a stony soil are its stone content (stoniness), water retention curves, and the hydraulic conductivity functions of both the soil matrix and rock fragments, as well as bulk characteristics representing the stony soil as a whole. Stoniness (R_v) is the ratio of the volume of rock fragments to the total volume of the soil.

The presence of stones can affect the hydraulic conductivity of a soil in several ways. On the one hand, stones reduce the effective cross-sectional area through which water flows, and combined with the fact that an increase in stoniness results in greater curvatures of flow paths, this can result in lower hydraulic conductivities (Bouwer and Rice, 1984; Childs and Flint, 1990; Ma et al., 2010; Novák et al., 2011; Ravina and Magier, 1984). In contrast, shrink-swell phenomena may create temporal lacunar pores (i.e., voids along the soil/stone interface) that can cause preferential flow and thus an increase in the saturated hydraulic conductivity (Sauer and Logsdon, 2002; Shi et al., 2008; Verbist et al., 2009; Zhou et al., 2009).

Rock fragments are relatively large compared to fine soil particles of the soil matrix. Therefore, it is necessary to evaluate the bulk soil characteristics for a "representative elementary volume" (REV) (Bear, 1972), the size of which depends mostly on the size and spatial distribution of the rock fragments. The larger the rock fragments are in the stony soil, the larger the REV needed. Buchter et al. (1994) recommended that the dry mass of a stony soil sample should be at least 100 times the mass of the largest particle. However, there is no rule for how large the REV of a stony soil should be for measuring its hydraulic characteristics. The dimension of the REV can vary from decimeters to meters, with its volume extending to about 1 m^3 when the rock fragments have a diameter of 10 cm or larger. The presence of rock fragments further presents problems for measuring the bulk soil hydraulic properties, water contents, water potential, or flow regime in general, due to such practical issues as the difficulty of inserting probes in stony soils (e.g., TDR probes and tensiometers) or installing lysimeters (Cousin et al., 2003; Ma et al., 2010).

Since it is technically difficult to perform hydraulic conductivity measurements on large samples with different stoniness, Novák et al. (2011) proposed the use of numerical models to simulate the classic Darcian flow experiment and to calculate the corresponding saturated hydraulic conductivity. This was done by embedding spherically shaped stones of different sizes (5, 10, and 20 cm in diameter) into a soil matrix of known hydraulic conductivity and then calculating the effective saturated hydraulic conductivity of the bulk sample with stones (K_s^b). Novák et al. (2011) showed that the effective hydraulic conductivity of a soil with a given stoniness is smaller when it contains a single "large" stone than when it contains multiple smaller stones. However, they only considered circular stones in the stoniness range of 0.07–0.31 $cm^3\ cm^{-3}$. From their study, it is not clear if the fine soil texture markedly affects simulated saturated hydraulic conductivities. However, their study indicated that one can similarly assess other factors that can potentially influence the hydraulic resistance to water flow such as different shapes, orientations, positions, and spatial distributions of rock fragments.

Therefore, the objective of this study is to describe and quantify the influence of stoniness and different shapes and positions of rock fragments on the bulk (effective) saturated hydraulic conductivity of stony soils using numerical modeling. This goal is achieved by answering the following questions:

1. How will A) the shape of rock fragments, B) the orientation of rock fragments, and C) the regular and irregular distributions of rock fragments affect the effective saturated hydraulic conductivity of stony soils?
2. How much will the effective saturated hydraulic conductivities of stony soils simulated using the numerical model differ from those calculated using existing empirical equations?
3. Is it possible to assess the effects of soil texture of the soil matrix on the effective saturated hydraulic conductivities of stony soils using a numerical model?
4. From simulated results, is it possible to propose a relationship between stoniness and the effective saturated hydraulic conductivity for different shapes, orientations, or distributions of rock fragments in a stony soil?

2. Theory

Only a few empirical equations for evaluating an effective saturated hydraulic conductivity of stony soils exist (e.g., Brakensiek et al., 1986; Ma et al., 2010; Ravina and Magier, 1984), and most are derived from laboratory experiments. The equation of Ravina and Magier (1984) is often used either in the absolute form to get the effective saturated hydraulic conductivity:

$$K_s{}^b = (1-R_v)K_s{}^f \tag{1}$$

or in the relative form to get the relative effective saturated hydraulic conductivity, K_{rs}:

$$K_{rs} = \frac{K_s{}^b}{K_s{}^f} = 1-R_v \tag{2}$$

where K_s^b and K_s^f are the effective saturated hydraulic conductivities of the bulk soil (denoted by index "*b*") and soil matrix (denoted by index "*f*"), respectively, and R_v is the relative volume of rock fragments in a stony soil (stoniness). According to Eq. (2), K_{rs} linearly decreases with an increasing relative volume of rock fragments. The use of this approach is recommended for sandy soils because their deformation due to water flow is not significant. The preliminary assumption is that properties of the soil matrix such as porosity are invariant with respect to the content of rock fragments.

The effective saturated hydraulic conductivity of a stony soil can also be calculated using the Corring and Churchill (1961) equations. Their equations were obtained from analytical solutions of heat transfer equations in dispersive environments. The equation for a stony soil with spherical rock fragments with a negligible or zero retention capacity that are dispersed in a soil matrix can be expressed as follows:

$$K_s{}^b = K_s{}^f\left(\frac{2(1-R_v)}{2+R_v}\right) \tag{3}$$

For cylindrical shaped rock fragments, it can be written as:

$$K_s{}^b = K_s{}^f\left(\frac{1-R_v}{1+R_v}\right) \tag{4}$$

Peck and Watson (1979) also derived an equation for spherical rock fragments identical to Eq. (3).

3. Methods

3.1. Numerical Darcy experiments

In this study, numerical Darcy experiments were performed in a similar fashion to Novák et al. (2011). A virtual stony soil was created by distributing rock fragments of different shapes and positions in the soil matrix, the hydraulic properties (i.e., the saturated hydraulic conductivity and the retention curve) of which were assumed to be known. Using HYDRUS (2D/3D) (Šimůnek et al., 2008), vertical water flow was then simulated in a vertical cross–section ($1 \times 1\ m^2$) with

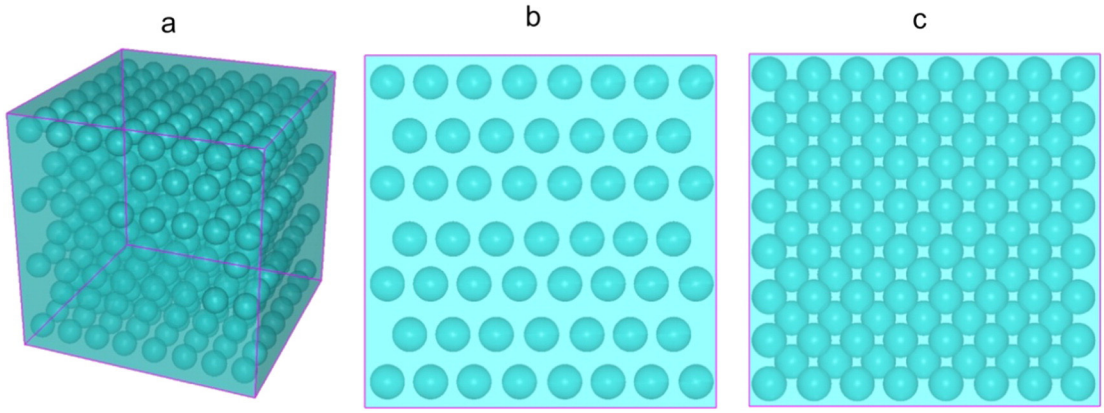

Fig. 1. Isometric view (a) and views in the x-(or y-) (b) and z-direction (c) of the three-dimensional transport domain with 403 regularly distributed spheres representing rock fragments (R_v of 0.211).

impermeable side walls. The final steady-state conditions were considered to represent steady-state water flow through a stony soil. Since the full saturation of the soil profile was considered as the initial condition, the steady-state conditions were reached very quickly; simulations had to be run for only about 90–150 min. To establish a unit pressure head gradient, the pressure head of 1 cm was applied at both the surface and bottom boundaries of a 1-m long soil profile. Consequently, the average water flux across the two boundaries was equal to the effective saturated hydraulic conductivity of a virtual stony soil.

Water movement in the virtual stony soil was simulated using the HYDRUS model, which numerically solves the Richards equation describing water flow in unsaturated and/or saturated porous media. This type of model is needed because both saturated and unsaturated regions are present in the flow domain, with unsaturated regions locally developing below rock fragments. The saturated soil water content, which corresponds to a zero pressure head, was used as the initial condition.

Several simplifying assumptions were made. It was assumed that the retention capacity and permeability of rock fragments were negligible, and that there was a close contact between rock fragments and the soil matrix [i.e., no lacunar pores (Fiès et al., 2002; Verbist et al., 2009) were present]. It was further assumed that water flow occurs only in the soil matrix (i.e., no flow through rock fragments) and that macropores and processes of solifluction and sealing can be neglected. Finally, it was assumed that flow through a fully three-dimensional system can be approximated using two-dimensional (2D) simulations. A limited number of fully three-dimensional simulations was carried out to evaluate the correspondence between results of two- and three-dimensional simulations.

Numerical experiments were divided into 3 scenarios. Scenario A represents regularly distributed RFs of different shapes (in cross-section circles, triangles, and ellipses), scenario B represents different orientations (horizontal or vertical) of slab-sided ellipses, and scenario C represents regularly and irregularly distributed spherical rock fragments. Dimensions of all rock fragment shapes are discussed below.

3.2. Shapes and orientations of rock fragments (scenarios A and B)

To assess the influence of rock fragment shapes on the saturated hydraulic conductivity of a virtual stony soil, rock fragments of different shapes, where 2D cross-sections are circles, ellipses, and triangles, were regularly distributed in a two-dimensional cross-section of the soil matrix. Two types of elliptical shapes were considered using the ratios of major and minor axes of 1.56 and 2.56. While the former elliptical shapes (ellipse No.1; the lengths of main axes were 4 and 6.25 cm) were only positioned horizontally (i.e., the major axis was horizontal), the latter elliptical shapes (ellipse No.2; the lengths of main axes were 3.125 and 8 cm) were positioned both horizontally and vertically. The base and height of triangles were 13 and 12.07 cm long, respectively. All circles, representing stones, were the same size, with a diameter of 10 cm. The cross-sectional area of 78.5 cm^2 was the same for all rock fragment shapes (i.e., circles, ellipses, and triangles). In three-dimensional simulations with regularly distributed spherical rock fragments, all spheres had a diameter of 10 cm and a volume of 523.6 cm^3.

In our numerical two-dimensional simulations, stoniness (R_v) is defined as the ratio of the cross-sectional area of rock fragments and the total cross-sectional area. It is assumed to be the same as the relative volume of rock fragments in the soil volume and was considered with values of 0.07, 0.16, 0.24, and 0.31 $cm^3\ cm^{-3}$. It was not technically possible to arrange the regular distribution of rock fragments for stoniness higher than 0.31 $cm^3\ cm^{-3}$, especially for triangular and ellipsoidal RFs. In the three-dimensional simulations, stoniness of 0.157 and 0.211 $cm^3\ cm^{-3}$ (corresponding with 300 and 403 rock fragments, respectively) was considered (Fig. 1). Simulations with zero stoniness represented soil samples without rock fragments. Hydraulic properties of the soil matrix, assumed to have the texture of either sandy loam, loam, or clay loam (Table 1), were taken from the soil catalog implemented in the HYDRUS software. These three textures were selected to represent a range of textures from coarse to fine.

3.3. Regular and irregular rock fragment distributions (scenario C)

Additional numerical experiments were performed to evaluate the influence of regular and irregular distributions of circular rock fragments in a stony soil on the effective saturated hydraulic conductivity K_s^b (and K_{rs}). Six different values of stoniness R_v (0.07, 0.16, 0.24, 0.31, 0.42, and 0.5 $cm^3\ cm^{-3}$) and eleven different spatial distributions of rock fragments were considered. While the first simulation assumed a regular distribution of rock fragments, the next ten simulations for each amount of stoniness considered irregular distributions of rock fragments. Irregular distributions of rock fragment positions were obtained using a random numbers pair generator. Generated coordinates of centers of circular rock fragments were adjusted so that rock fragments

Table 1
Soil hydraulic parameters for the analytical model of van Genuchten (1980) for three textural classes of the USDA soil textural triangle according to Carsel and Parrish (1988) (taken from the HYDRUS soil catalog).

Textural class	θ_r ($cm^3\ cm^{-3}$)	θ_s ($cm^3\ cm^{-3}$)	α (cm^{-1})	n (−)	K_s^f ($cm\ h^{-1}$)
Sandy Loam	0.065	0.41	0.075	1.89	4.42
Loam	0.078	0.43	0.036	1.56	1.04
Clay Loam	0.095	0.41	0.019	1.31	0.26

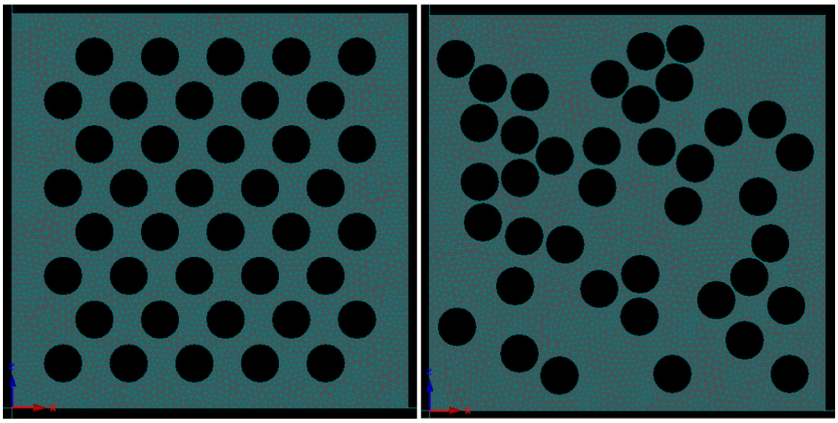

Fig. 2. Examples of regular and irregular distributions of rock fragments in a stony soil with a stoniness R_v of 0.31 cm^3cm^{-3}.

were not overlapping or in contact with each other. Examples of regular and irregular distributions of rock fragments are shown in Fig. 2. Since no significant differences were observed between results of simulations evaluating the effect of the spatial distribution of rock fragments when different fine soil textures were considered to represent the soil matrix, only results for sandy loam are reported below.

Results of numerical experiments with respect to effective hydraulic conductivities for corresponding stoniness were evaluated in relative values. Mean values (for all scenarios, with different shapes, orientations, and distributions of RFs for a given stoniness) and their standard deviations (for scenario C), as well as the range of values (min and max) for scenarios A and B, together with 95% confidence intervals for scenario C, were estimated. Confidence intervals (± 2 standard deviations) were calculated from eleven discrete values for every considered stoniness, assuming Gaussian distribution of simulated K_{rs} values. Furthermore, the relative effective saturated hydraulic conductivities simulated for all scenarios were compared with values calculated according to both Ravina and Magier (1984) (Eq. (2); RM), and Corring and Churchill (1961) for spherical (Eq. (3); CCS) and cylindrical (Eq. (4); CCC) shapes of RFs, divided by a corresponding saturated hydraulic conductivity of the soil matrix. Decreases or increases of simulated values of relative effective saturated hydraulic conductivities were expressed in percentages of calculated values. The effects of shape, orientation, or distribution of rock fragments and stoniness on the relative saturated hydraulic conductivity were assessed using a linear or nonlinear regression.

4. Results

The results presented in the following sections refer to two-dimensional simulations, unless specified otherwise.

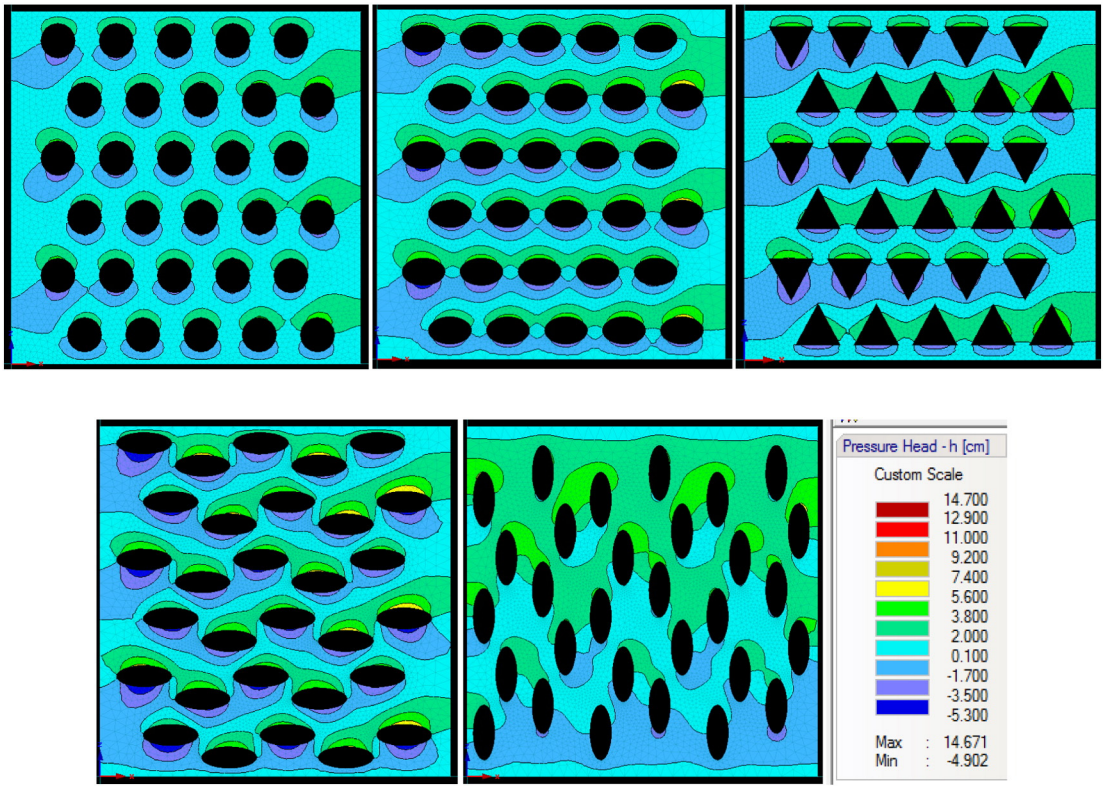

Fig. 3. Spatial distributions of pressure heads (cm) in soils with rock fragments regularly distributed in the sandy loam matrix and a stoniness R_v of 0.24 cm^3cm^{-3}. Water flow is from top to bottom.

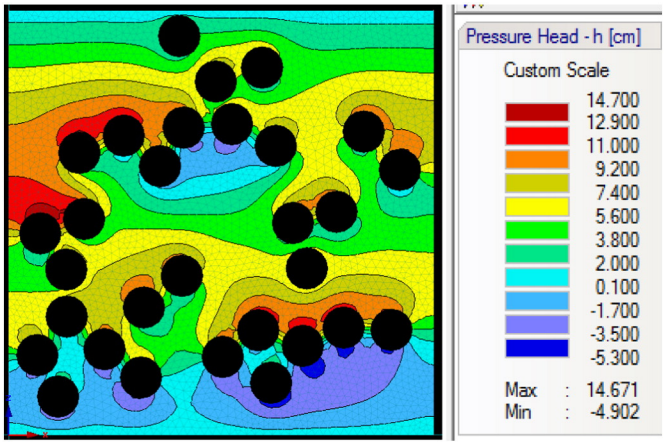

Fig. 4. The spatial distribution of pressure heads (cm) in a soil with rock fragments irregularly distributed in the sandy loam matrix and a stoniness R_v of 0.24 cm^3cm^{-3}. Water flow is from top to bottom.

4.1. Spatial distributions of pressure heads, water contents, and water fluxes

Spatial distributions of pressure heads, volumetric soil water contents, and water fluxes in soils with rock fragments either regularly or irregularly distributed in the soil matrix are presented in Figs. 3–9. Spatial distributions of pressure heads (Figs. 3 and 4) show that there are indeed regions immediately above rock fragments with positive pressure heads greater than the boundary pressure head of 1 cm. Immediately below rock fragments, there are regions with negative pressure heads, indicating unsaturated conditions. This phenomenon was observed in all simulations with RFs. The minimum and maximum differences in pressure heads for regularly distributed rock fragments were observed for elliptic rock fragments oriented vertically and horizontally, respectively. The maximum differences in pressure heads were observed for conditions with an irregular distribution of rock fragments. The maximum and minimum pressure heads of 14.6 cm and −4.9 cm, respectively, were observed in the soil with stoniness of 0.24 cm^3 cm^{-3} and the sandy loam soil matrix (Fig. 4).

Almost entire soil systems, with the exception of small regions immediately below the rock fragments, were fully saturated. The extent of the unsaturated regions depended on the shape of rock fragments. While the unsaturated regions were very small, or sometimes even did not develop, for spherical and elliptical (oriented vertically) rock fragments, larger unsaturated regions developed below elliptical, horizontally oriented rock fragments or triangular rock fragments. Similarly as for pressure heads, the greatest differences in soil water contents were observed for conditions with an irregular distribution of rock fragments (Fig. 6).

Non–uniform water fluxes (Figs. 7–8) were the consequence of non-uniform pressure head distributions (Figs. 3–4). Water fluxes were smallest (approaching zero) immediately above and below the rock fragments. They were significantly larger (by up to 50%) than the saturated hydraulic conductivity between the rock fragments. The largest water fluxes were observed for conditions with an irregular distribution of rock fragments (Fig. 8).

Fig. 9 compares the spatial distribution of water fluxes in a soil with regularly distributed rock fragments in a two- and three-dimensional simulations. A cross-section through the middle of the domain is shown for a three-dimensional simulation. While a two-dimensional domain contains 8 rows of rock fragments, a cross-section through a three-dimensional domains contains only 4 rows, since the other 4 rows were moved in the *y*-direction. A similar patterns of water fluxes is apparent around rock fragments present in the cross-section. Note that the largest fluxes in a three-dimensional simulation were calculated for regions with 'missing' (moved) rock fragments, where flow was accelerated at the surface of these fragments.

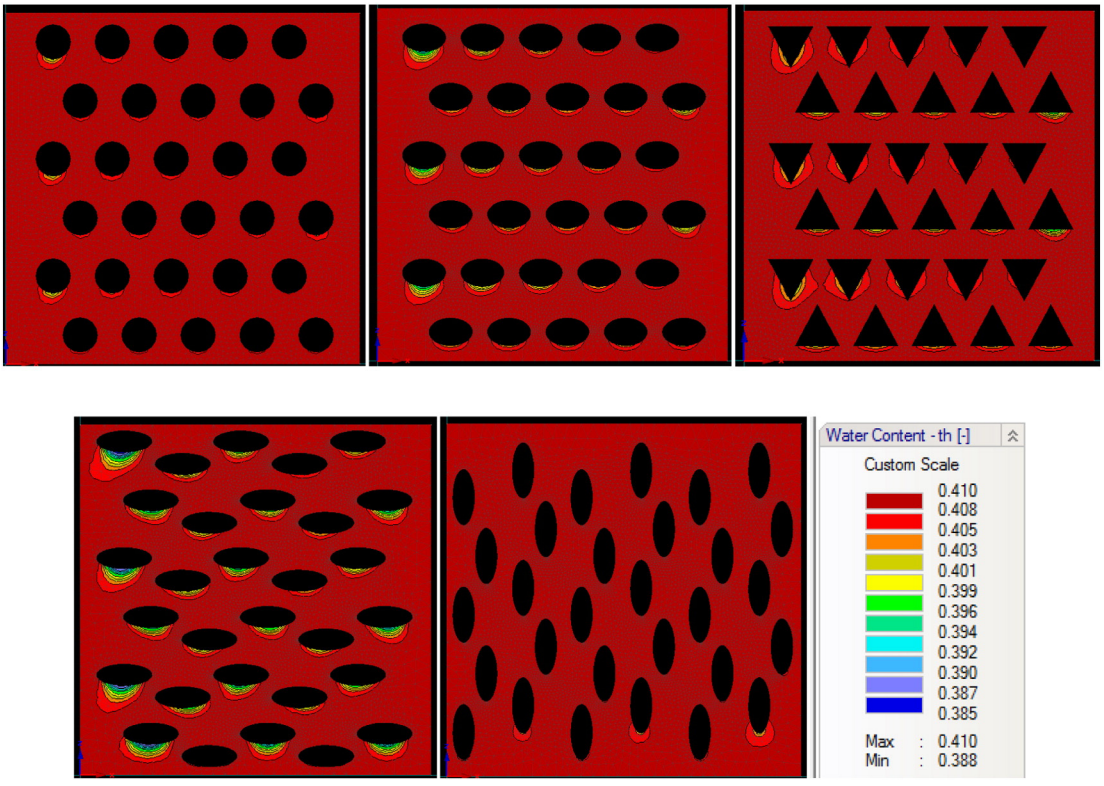

Fig. 5. Spatial distributions of volumetric soil water contents in soils with rock fragments regularly distributed in the sandy loam matrix and a stoniness R_v of 0.24 cm^3cm^{-3}. Water flow is from top to bottom.

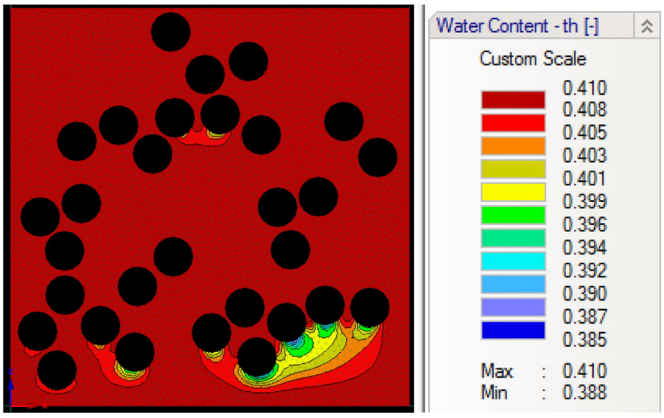

Fig. 6. The spatial distribution of volumetric soil water contents in a soil with rock fragments irregularly distributed in the sandy loam matrix and a stoniness R_v of 0.24 cm^3cm^{-3}. Water flow is from top to bottom.

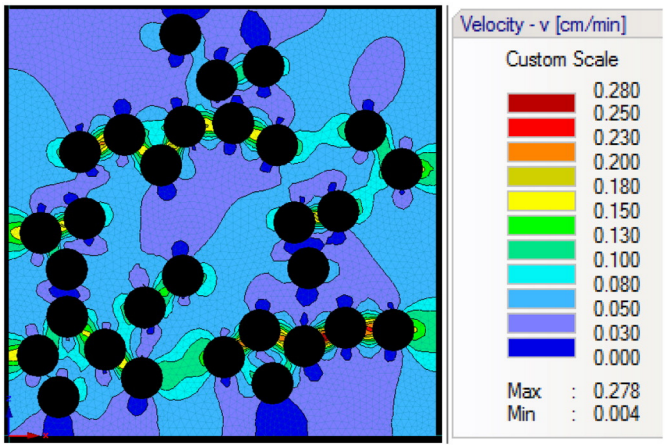

Fig. 8. The spatial distribution of water fluxes (cm/min) in a soil with rock fragments irregularly distributed in the sandy loam matrix and a stoniness R_v of 0.24 cm^3cm^{-3}. Water flow is from top to bottom.

All simulated scenarios indicate that the effective or relative saturated hydraulic conductivities always decrease with increasing stoniness. The decrease in hydraulic conductivities depends not only on stoniness, but also on the shape, orientation, and distribution of rock fragments in the soil, as well as on the texture of the soil matrix, as discussed in more detail below.

4.2. Relative effective saturated hydraulic conductivities

4.2.1. The effect of shapes and orientations of rock fragments (scenarios A and B)

The largest K_{rs} values for all simulated stoniness were obtained for slab-sided ellipses (No. 2) oriented vertically, followed by circles, triangles, and No.1 ellipses. The smallest K_{rs} values were obtained for slab-sided ellipses (No. 2) horizontally oriented. These trends in K_{rs} are displayed in Fig. 10a, together with linear regression equations expressing the dependence of K_{rs} on stoniness R_v.

While mean K_{rs} values for scenarios A and B were almost identical, their smallest and largest values were different (Table 2). The effect of similarly shaped rock fragments in scenario A on the smallest and largest K_{rs} values was smaller than the effect of the orientation of slab-sided ellipses in scenario B. The difference between the largest and smallest K_{rs} values due to different orientations of the same elliptical rock fragments is quite large. For example, for a stoniness of 0.24 cm^3 cm^{-3}, the difference between K_{rs} of a system with elliptical rock fragments either horizontally or vertically oriented was 0.26 (the range of values for scenario B) (Table 2, Fig. 10a, ellipses denoted as "2-H" or "2-V"). In

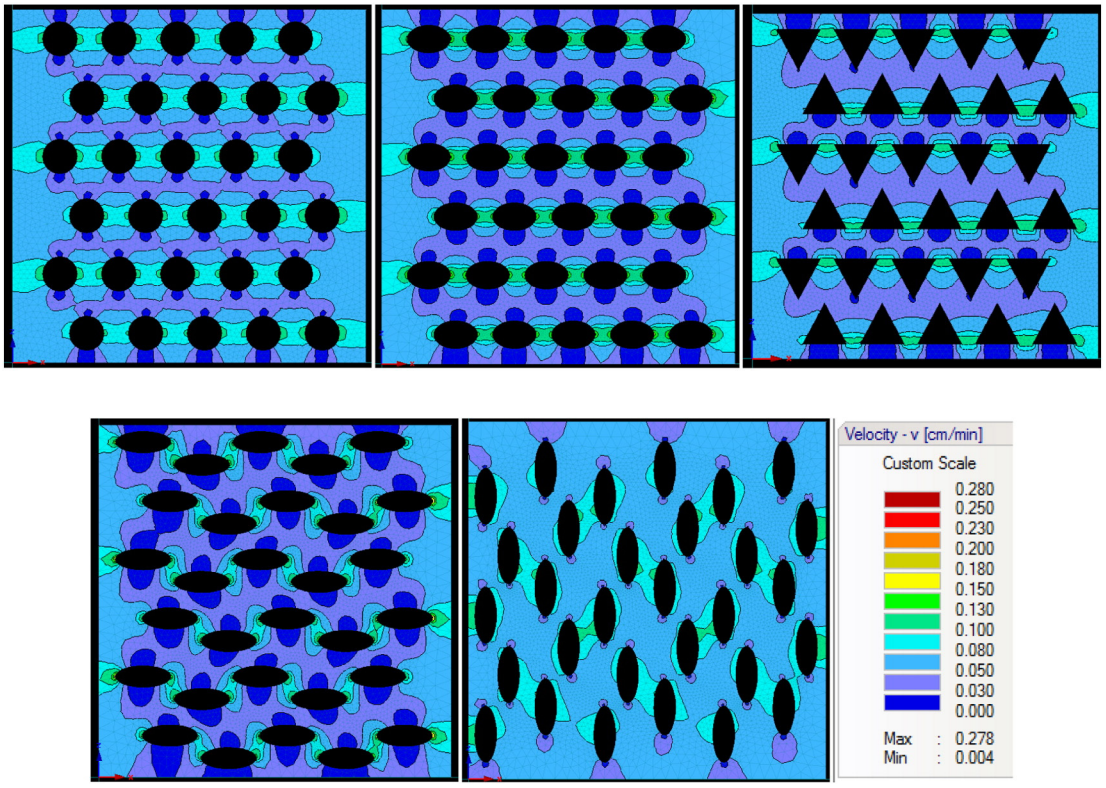

Fig. 7. Spatial distributions of water fluxes (cm/min) in soils with rock fragments regularly distributed in the sandy loam matrix and a stoniness R_v of 0.24 cm^3cm^{-3}. Water flow is from top to bottom.

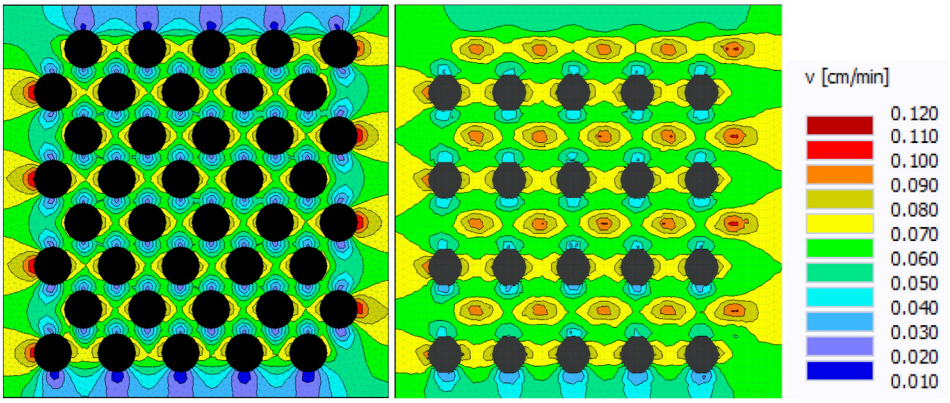

Fig. 9. Comparison of the spatial distributions of water fluxes (cm/min) in a soil with rock fragments regularly distributed in the sandy loam matrix in two-dimensional (a stoniness R_v of 0.31 cm^3cm^{-3}) (left) and three-dimensional (a stoniness R_v of 0.211 cm^3cm^{-3}) (right) systems. Water flow is from top to bottom.

contrast, the difference between the smallest and largest K_{rs} values for soils with different rock fragment shapes in scenario A (circles, triangles, and ellipses with small axes ratio, denoted in Fig. 10a as "1-H″) for a stoniness of 0.24 $cm^3\ cm^{-3}$ was only 0.11.

Numerical experiments indicated that the reduction in the relative effective saturated hydraulic conductivity K_{rs} as a function of stoniness R_v does not depend on hydraulic properties of the soil matrix. Although the results displayed in Fig. 10a are only for a sandy loam matrix, almost identical results were obtained for the other two soil matrix textures. Numerical experiments further indicated that the relative effective saturated hydraulic conductivity K_{rs} decreases much faster as a function of stoniness R_v than predicted by the equation of Ravina and Magier (1984) and that this decrease depends on the shape and orientation of rock fragments. Therefore, we generalized the equation of Ravina and Magier (1984) for different shapes and orientations of rock fragments as follows:

$$K_{rs} = \frac{K_s^{\ b}}{K_s^{\ f}} = b - a.R_v \tag{5}$$

and the following parameters a and b (Fig. 10a) were fitted using linear regression for:

1. spherical rock fragments with a diameter of 10 cm: $a = 1.45$, $b = 0.97$ with $r^2 = 0.98$,
2. ellipsoidal rock fragments with a long axis of 4 and 6.25 cm and triangular rock fragments with a height of 12.07 cm and a base of 13 cm: $a = 1.75$, $b = 0.96$ with $r^2 = 0.98$,
3. ellipsoidal rock fragments with a long axis of 3.125 and 8 cm vertically oriented: $a = 1.23$, $b = 0.99$ with $r^2 = 0.99$, and
4. ellipsoidal rock fragments with a long axis of 3.125 and 8 cm horizontally oriented: $a = 1.98$, $b = 0.92$ with $r^2 = 0.93$.

Simulated relative effective saturated hydraulic conductivities were either underestimated or overestimated in comparison with calculated values. This under- or over-estimation depends on a) the calculation method, b) the modeled scenario, and c) stoniness. The relative deviations in percentages between simulated and calculated values are presented in Table 3.

Simulated values of K_{rs} were underestimated in all scenarios compared with the Ravina and Magier (1984) function (RM), which also predicts a smaller decrease of K_{rs} as a function of stoniness than both equations of Corring and Churchill (1961). With respect of the effect of the shapes of RFs (scenario A), the smallest deviations between modeled and calculated values were obtained for the Corring and

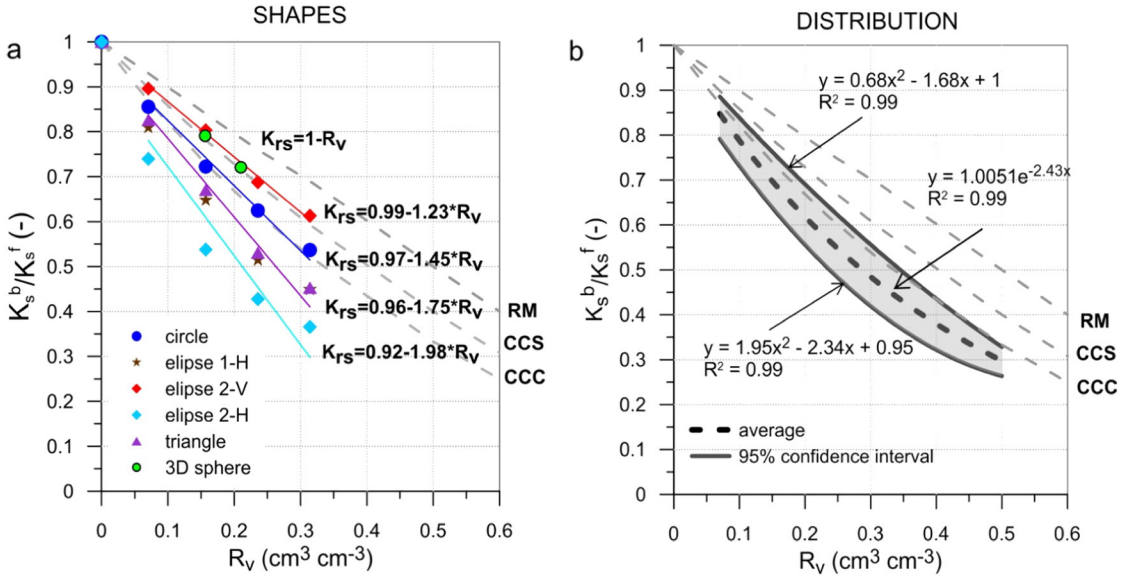

Fig. 10. The relative saturated hydraulic conductivity ($K_{rs} = K_s^b/K_s^f$) as a function of stoniness R_v and the shape of rock fragments (Fig. 10a, symbols V and H denote vertical and horizontal positioning of ellipses, respectively) and the spatial distribution of circular rock fragments (Fig. 10b). All results were obtained using the two-dimensional simulations, except for "3D sphere", which were obtained using the three-dimensional simulations. Relationships denoted as RM, CCS, and CCC were calculated according to *Ravina and Magier* (1984); *Corring and Churchill* (1961) for spheres, and *Corring and Churchill* (1961) for cylinders, respectively. Results are displayed for a sandy loam matrix.

Table 2
Mean, smallest and largest K_{rs} values, as well as the range of relative effective saturated hydraulic conductivities of stony soils for different modeling scenarios.

Stoniness, R_v	Mean values[a]							Smallest and largest values[b], /range/					
	0	**0.07**	**0.16**	**0.24**	**0.31**	**0.42**	**0.5**	**0.07**	**0.16**	**0.24**	**0.31**	**0.42**	**0.5**
	K_{rs}, relative values							K_{rs}, relative values					
Regularly dist. RF. Scenario A	1	0.83	0.68	0.56	0.48	–	–	0.81–0.86 /0.05/	0.65–0.72 /0.07/	0.51–0.62 /0.11/	0.45–0.54 /0.09/	–	–
Regularly dist. RFs Scenario B	1	0.82	0.67	0.56	0.49	–	–	0.74–0.9 /0.16/	0.54–0.8 /0.26/	0.43–0.69 /0.26/	0.37–0.61 /0.24/	–	–
								95% Confidence interval					
Reg. & irr. dist. RFs Scenario C	1 (0)	0.832 (0.023)	0.698 (0.030)	0.570 (0.036)	0.460 (0.038)	0.365 (0.019)	0.297 (0.020)	0.785–0.878 /0.093/	0.638–0.758 /0.12/	0.497–0.643 /0.146/	0.384–0.537 /0.153/	0.327–0.402 /0.075/	0.257–0.337 /0.08/

Scenario A represents regularly distributed RFs of different shapes: circles (diameter 10 cm), triangles (base 13 cm, height 12.07 cm), ellipses (main axes 4 cm and 6.25 cm).
Scenario B represents different orientations of the ellipses (with main axes 3.125 cm and 8 cm); the minimum values are for RFs oriented horizontally, the maximum values are for RFs oriented vertically.
Scenario C represents regularly and irregularly distributed spherical RF (diameter 10 cm).
[a] In parentheses are standard deviations.
[b] Smallest and largest values in scenarios A and B, in scenario C they correspond to 95% confidence intervals.

Table 3
Differences (%) between simulated relative effective saturated hydraulic conductivities of stony soils and their corresponding values calculated from an empirical equation for stoniness from 0.07 to 0.5 cm cm^{-3}. Positive values indicate that simulated values were larger than calculated values. RM denotes to Ravina and Magier (1984) function, CCS denotes to Corring and Churchill (1961) function (for spheres), CCC denotes to Corring and Churchill (1961) function (for cylinders).

Stoniness, R_v		Mean values							Smallest and largest values					
		0	**0.07**	**0.16**	**0.24**	**0.31**	**0.42**	**0.5**	**0.07**	**0.16**	**0.24**	**0.31**	**0.42**	**0.5**
		Relative differences (in %) between simulated and calculated K_{rs} values according to particular equations (RM, CCS or CCC)												
									Min (max)					
Regularly dist. RFs Scenario A	RM	0.0	−10.8	−19.0	−26.3	−30.4	–	–	−12.9 (−7.5)	−22.6 (−14.3)	−32.9 (−18.4)	−34.8 (−21.7)	–	–
	CCS	0.0	−7.6	−12.6	−17.5	−19.7	–	–	−9.9 (−4.3)	−16.4 (−7.4)	−24.8 (−8.6)	−24.7 (−9.6)	–	–
	CCC	0.0	−4.5	−6.1	−8.6	−8.9	–	–	−6.8 (−1.1)	−10.2 (−0.6)	−16.8 (1.2)	−14.6 (2.5)	–	–
		0.0							Min (max)[a]					
Regularly dist. RFs Scenario B	RM	0.0	−11.8	−20.2	−26.3	−29.0	–	–	−20.4 (−3.2)	−35.7 (−4.8)	−43.4 (−9.2)	−46.4 (−11.6)	–	–
	CCS	0.0	−8.7	−13.9	−17.5	−18.0	–	–	−17.6 (0.2)	−30.6 (2.9)	−36.6 (1.7)	−38.1 (2.1)	–	–
	CCC	0.0	−5.7	−7.5	−8.6	−7.0	–	–	−14.9 (3.5)	−25.4 (10.5)	−29.8 (12.6)	−29.8 (15.8)	–	–
		0.0							95% Confidence interval, min (max)					
Rreg. & irr. dist. RFs Scenario C	RM	0.0	−10.5	−16.9	−25.0	−33.3	−37.1	−40.6	−15.6 (−5.6)	−24.0 (−9.8)	−34.6 (−15.4)	−44.3 (−22.2)	−43.6 (−30.7)	−48.6 (−32.6)
	CCS	0.0	−7.4	−10.3	−16.0	−23.0	−23.9	−25.8	−12.6 (−2.3)	−18.0 (−2.5)	−26.8 (−5.2)	−35.7 (−10.1)	−31.8 (−16.1)	−35.8 (−15.8)
	CCC	0.0	−4.3	−3.6	−7.0	−12.7	−10.6	−10.9	−9.7 (1.0)	−11.9 (4.7)	−18.9 (4.9)	−27.1 (2.0)	−19.9 (−1.6)	−22.9 (1.1)

[a] The smallest values correspond to RFs oriented horizontally, the largest values correspond to RFs oriented vertically.

Churchill (1961) equation for cylindrical RFs (CCC). Compared with the RM method, the K_{rs} values for soils with spherical rock fragments were underestimated by 7–21% in the stoniness range of 0.07–0.31 $cm^3\ cm^{-3}$. Whereas the K_{rs} values were only underestimated by 4–9% compared to the Corring and Churchill (1961) equation for spherical RFs (CCS). Compared to the Corring and Churchill (1961) equation for cylindrical RFs (CCC), the K_{rs} values were either underestimated by 1.1–0.6% in the range of stoniness of 0.07–0.16 $cm^3\ cm^{-3}$, or overestimated by 1.2–2% in the range of stoniness of 0.24–0.31 $cm^3\ cm^{-3}$.

The good agreement between K_{rs} values predicted by the Corring and Churchill (1961) equation for cylindrical RFs (CCC) and the two-dimensional simulations with spherical rock fragments is not surprising. While the goal of these simulations was to evaluate the effects of spherical rock fragments, the two-dimensional simulations can only consider a circular projections of these fragments and neglect the effects of the third direction. These calculations thus indeed simulate the effects of cylindrical, rather than spherical, rock fragments. On the other hand, the results of the three-dimensional simulations, which could fully account for spherical shapes of the rock fragments, corresponded closely with values predicted by the Corring and Churchill (1961) equation for spherical RFs (CCS) (Fig. 10a). The good agreement between the results of both two- and three-dimensional simulations with cylindrical and spherical rock fragments, respectively, with the Corring and Churchill (1961) equations confirms the robustness of these equations, as well as the correctness of our numerical simulations.

The K_{rs} values of stony soils with slab-sided elliptical RFs were underestimated for the entire range of stoniness of 0.07–0.31 $cm^3\ cm^{-3}$ compared with all calculation methods when RFs were horizontally oriented. These values represented the minimum K_{rs} values for scenario B. When RFs were vertically oriented, the K_{rs} values corresponded to the maximum K_{rs} values for scenario B. In this case, the K_{rs} values were only underestimated when compared to the RM equation (by 3–11%), and overestimated when compared to the CCS or CCC methods (by 0.2–2.1% and 3.5–15.8%, respectively).

4.2.2. The effect of regular and irregular distributions of rock fragments (scenario C)

The largest K_{rs} values for scenarios with irregularly distributed RFs were for all amounts of stoniness close to the K_{rs} values when rock fragments were regularly distributed. The mean K_{rs} values for scenario C in the range of stoniness of 0.07–0.31 $cm^3\ cm^{-3}$ were almost the same as the mean values for scenarios A and B. The confidence intervals show an overlap between the minimum K_{rs} values for a particular stoniness and the maximum K_{rs} values for the next higher stoniness.

The mean and largest and smallest K_{rs} values for scenario C were fitted using non-linear regression polynomial functions (Fig. 10b). The largest K_{rs} values were similar to those for scenario A for regularly distributed spherical shaped RFs (Table 2). The difference between the largest and smallest K_{rs} values due to regular and irregular distributions of RFs varied from 0.075 to 0.153 in the range of stoniness of 0.07–0.5 $cm^3\ cm^{-3}$, with the largest difference identified at a stoniness of 0.31 $cm^3\ cm^{-3}$. Table 2 summarizes the mean K_{rs} values, their standard deviations, and 95% confidence intervals (the mean value ± 2 times the standard deviation) for different classes of stoniness.

The mean and smallest K_{rs} values were always underestimated in this scenario compared to all calculation methods (Table 3). The largest K_{rs} values were underestimated compared to the RM and CCS methods. Compared to the Corring and Churchill (1961) equation for cylindrical RFs (CCC), the largest K_{rs} values were almost always overestimated (by 1–4.9%) in the range of stoniness of 0.07–0.5 $cm^3\ cm^{-3}$, except for a stoniness of 0.42 $cm^3\ cm^{-3}$ when a small underestimation (by 1.6%) was found.

Results in Figs. 10a and b are shown only for stoniness smaller than 0.31 or 0.5 $cm^3\ cm^{-3}$, respectively, since it was difficult to regularly or irregularly distribute rock fragments of all shapes for a larger stoniness. The presence of rock fragments decreased the cross-sectional area of the soil through which water flows and correspondingly, the relative saturated hydraulic conductivity, as expressed by Eq. (2) of Ravina and Magier (1984). The shape, orientation and spatial distribution of rock fragments provided an additional influence on the curvatures of water flow paths and consequently, the resistance to water flow through the soil.

5. Discussion

Due to many factors such as the required size of the REV for stony soils, as discussed by Novák et al. (2011), it is difficult to compare values calculated using numerical experiments with measured values. Empirical evidence for the effect of the size of rock fragments on stony soil saturated hydraulic conductivity was presented by Novák et al. (2011). For example, Novák et al. (2011) showed that large rock fragments with a diameter of 20 cm decreased the relative effective saturated hydraulic conductivity more than smaller rock fragments with diameters of 10 or 5 cm with the same total volume. Similarly, Ma and Shao (2008), for RFs with diameters in the range of 5–40 mm, showed a more significant decrease in the infiltration rate due to larger rock fragments than due to a larger number of smaller stones of the same volume. They also pointed out that rock fragments of a spherical shape decrease the infiltration rate less than rock fragments of cylindrical or prismatic shapes. Ma and Shao (2008) explained this phenomenon by different resistances to water flow for differently shaped rock fragments.

Using field measurements, Verbist et al. (2009) observed both a decrease and an increase in K_s^b with stoniness. Stoniness was expressed in their study using different measures such as a relative volume, a relative mass, or a mean weighted diameter of rock fragments. Increasing or decreasing trends, with moderate (correlation coefficients equal to 0.51–0.63) and weak (correlation coefficients equal to 0.14–0.19) correlations, respectively, were the result of two opposing phenomena: 1) rock fragments causing greater curvature of flow paths and a decrease in K_s^b, and 2) the presence of interconnected lacunar pores or other macropores causing an increase in K_s^b. Verbist et al. (2013) further showed that the saturated hydraulic conductivity of a stony soil determined in the field can be highly variable, not only because of soil heterogeneity, but also due to the measurement method, the number of replications, and the calculation method. Furthermore, it is not clear how much different measurement results are affected by the stony character of the soil or different measurement methods.

Since the possible presence of lacunar pores (or macropores) was not accounted for in our numerical experiments, calculated K_s^b values are decreasing with increasing stoniness. Calculated values of K_s^b are always lower than those calculated according to Ravina and Magier (1984). One reason for this may be that Eq. (1) or (2) of Ravina and Magier (1984) do not consider the influence of additional resistances caused by different shapes, orientations, and positions of rock fragments.

Our numerical simulations that evaluated irregular distributions of rock fragments did not consider situations when rock fragments were in contact with each other. In such a situation, not only the influence of the position of rock fragments on K_s^b would be evaluated, but also their size effect, since such rock fragments would behave as larger stones, which had already been evaluated in an earlier study (Novák et al., 2011). In addition, situations when all rock fragments are concentrated in one part of the flow domain were not considered.

Shapes and positions of rock fragments can have a significant influence on the hydrophysical properties of stony soils. This can be especially manifested for saturated conditions. The distribution and orientation of rock fragments in mountainous areas are strongly affected by the process of pedogenesis, slope gradient, and topographic position (Chen et al., 2011, 2012). Rock fragments can be oriented parallel with the slope. Consequently, such soils can have different hydraulic conductivities in horizontal and vertical directions, producing macroscopic

anisotropy. This anisotropic behavior can, for example, accelerate hypodermic flow at the hillslope scale and speed up the formation of subsurface flow (Capuliak et al., 2010).

Water flow in stony soils is a complex, three-dimensional phenomenon. Therefore, since majority of numerical experiments, the results of which were discussed above, have been carried out using a two-dimensional model, the results are only approximate. Nevertheless, we anticipate, as was partially confirmed by a limited number of three-dimensional simulations reported above, that differences between our estimated hydraulic conductivities and those that would be estimated using a fully three-dimensional model would be small, and that the general relationships and various trends discussed above would be preserved.

6. Conclusions

Numerical experiments showed that the effective hydraulic conductivity of saturated stony soils K_s^b decreased as stoniness increased. However, the K_s^b estimates depended not only on stoniness (R_v) as previously shown by others such as Ravina and Magier (1984), but they were also sensitive to other factors such as the shape, distribution, and orientation of the rock fragments in stony soils. For example, the largest (0.9, 0.8, 0.69, 0.61) and smallest (0.74, 0.54, 0.43, 0.37) values of the relative saturated hydraulic conductivities K_{rs} for stoniness of 0.07, 0.16, 0.24, and 0.31 $cm^3\ cm^{-3}$ were estimated for rock fragments of elliptical shape that were either vertically or horizontally oriented, respectively. The Ravina and Magier (1984) function (RM) unpredicted a decrease of K_{rs} as a function of stoniness compared to the results of numerical simulations for all shapes, orientations, and distributions of rock fragments, as well as compared to both equations of Corring and Churchill (1961). Therefore, we have generalized the equation of Ravina and Magier (1984) to account for the shape and orientation of rock fragments and identified the values of additionally required parameters a and b.

The results of the two-dimensional simulations with circular inclusions agreed well with the K_{rs} values predicted by the Corring and Churchill (1961) equation for cylindrical RFs (CCC). Similarly, the results of the three-dimensional simulations with spherical shapes of the rock fragments corresponded closely with values predicted by the Corring and Churchill (1961) equation for spherical RFs (CCS). The good agreement between the results of both two- and three-dimensional simulations with cylindrical and spherical rock fragments with the Corring and Churchill (1961) equations confirms the robustness of these equations in describing the effects of rock fragments of specific shapes on the hydraulic conductivity of stony soils, as well as the correctness of our numerical simulations.

The relative effective saturated hydraulic conductivities K_{rs} also depended on whether the rock fragments were regularly or irregularly distributed in a stony soil. The largest difference of 0.153 in K_{rs} estimates due to irregular distribution of rock fragments in the stony soil was obtained for a stoniness of 0.31 $cm^3\ cm^{-3}$. Differences in K_{rs} estimates due to irregular distributions of rock fragments decreased for both large (0.5 $cm^3\ cm^{-3}$) and small (0.07 $cm^3\ cm^{-3}$) stoniness.

Finally, results of steady-state water flow simulations indicated that the relative saturated hydraulic conductivities K_{rs} do not depend on the hydraulic properties of the soil matrix of stony soils for a particular shape and orientation of rock fragments.

Acknowledgements

We are grateful to two anonymous reviewers for their careful reviews of our manuscript, all their editorial suggestions and requests for clarifications, and for their guidance in helping us to significantly improve our manuscript.

This contribution was partially supported by a grant from the Slovak Academy of Sciences VEGA (project No. 2/0055/15, No. 2/0013/15), and is the result of the project implementation ITMS 26240120004 from the Centre of Excellence for Integrated Flood Protection of Land, as supported by the Research & Development Operational Program funded by the European Regional Development Fund.

References

Al-Qinna, M., Scott, H.D., Brye, K.R., Brahana, J.V., Sauer, T.J., Sharpley, A., 2014. Coarse fragments affect soil properties in a mantled-karst landscape of the Ozark Highlands. Soil Sci. 179, 42–50.
Bear, J., 1972. Dynamics of Fluids in Porous Media. American Elsevier, New York.
Bouwer, H., Rice, R.C., 1984. Hydraulic properties of stony vadose zones. Ground Water 22, 696–705.
Brakensiek, D.L., Rawls, W.J., Stephenson, G.R., 1986. Determining the saturated hydraulic conductivity of a soil containing rock fragments. Soil Sci. Soc. Am. J. 50, 834–835.
Brouwer, J., Anderson, H., 2000. Water holding capacity of ironstone gravel in typic Phlintoxeralf in Southeast Australia. Soil Sci. Soc. Am. J. 64, 1603–1608.
Buchter, B., Hinz, C., Flühler, H., 1994. Sample size for determination of coarse fragment content in a stony soil. Geoderma 63, 265–275.
Capuliak, J., Pichler, V., Flühler, H., Pichlerová, M., Homolák, M., 2010. Beech forest density control on the dominant water flow types in andic soils. Vadose Zone J. 9, 755–769.
Carsel, R.F., Parrish, R.S., 1988. Developing joint probability distributions of soil water retention characteristics. Water Resour. Res. 24, 755–769.
Chen, H., Liu, J., Wang, K., Zhang, W., 2011. Spatial distribution of rock fragments on steep hillslopes in karst region of northwest Guangxi, China. Catena 84, 21–28.
Chen, H., Liu, J., Zhang, W., Wang, K., 2012. Soil hydraulic properties on the steep karst hillslopes in northwest Guangxi, China. Environ. Earth Sci. 66, 371–379.
Childs, S.W., Flint, A.L., 1990. Physical properties of forest soils containing rock fragments. In: Gessel, S.P., Lacate, D.S., Weetman, G.F., Powers, R.F. (Eds.), Sustained Productivity of Forest Soils, Proceedings of the 7th North American Forest Soils Conference. University of British Columbia, Faculty of Forestry Publication, Vancouver, pp. 95–121.
Corring, R.L., Churchill, S.W., 1961. Chem. Eng. Prog. 57, 53–59.
Cousin, I., Nicollaud, B., Coutadeur, C., 2003. Influence of rock fragments on the water retention sand and water percolation in a calcareous soil. Catena 53, 97–114.
Fiès, J.C., De Louvigny, N., Chanzy, A., 2002. The role of stones in soil water retention. Eur. J. Soil Sci. 53, 95–404.
Hlaváčiková, H., Novák, V., Holko, L., 2015. On the role of rock fragments and initial soil water content in the potential subsurface runoff formation. J. Hydrol. Hydromech. 63, 71–91.
Hraško, J., Bedrna, Z., 1988. Applied Soil Science. Priroda Publ. House, Bratislava (in Slovak).
Ma, D.H., Shao, M., 2008. Simulating infiltration into stony soils with a dual-porosity model. Eur. J. Soil Sci. 59, 950–959.
Ma, D.H., Shao, M.A., Zhang, J.B., Wang, Q.J., 2010. Validation of an analytical method for determining soil hydraulic properties of stony soils using experimental data. Geoderma 159, 262–269.
Novák, V., Kňava, K., Šimůnek, J., 2011. Determining the influence of stones on hydraulic conductivity of saturated soils using numerical method. Geoderma 161, 177–181.
Peck, A.J., Watson, J.D., 1979. Hydraulic Conductivity and Flow in Non-Uniform Soil. Worshop on Soil Physics and Soil Heterogeneity. CSIRO Division of Environmental Mechanics, Canberra, Australia.
Poesen, J., Lavee, H., 1994. Rock fragments in top soils: significance and processes. Catena 23, 1–28.
Ravina, I., Magier, J., 1984. Hydraulic conductivity and water retention of clay soils containing coarse fragments. Soil Sci. Soc. Am. J. 48, 736–740.
Šály, R., 1978. Soil - Basic Component of Forest Production. Priroda Publ. House, Bratislava (in Slovak).
Sauer, T.J., Logsdon, S.D., 2002. Hydraulic and physical properties of stony soils in a small watershed. Soil Sci. Soc. Am. J. 66, 1947–1956.
Shi, Z., Wang, Y., Yu, P., Xu, L., Xiong, W., Guo, H., 2008. Effect of rock fragments on the percolation and evaporation of forest soil in Liupan Mountains, China. Acta Ecol. Sin. 28, 6090–6098.
Šimůnek, J., van Genuchten, M.T., Šejna, M., 2008. Development and applications of the HYDRUS and STANMOD software packages and related codes. Vadose Zone J. 7, 587–600. http://dx.doi.org/10.2136/vzj2007.0077.
van Genuchten, M.T., 1980. A closed – form equation for predicting the hydraulic conductivity of unsaturated soils. Soil Sci. Soc. A. J. 44, 987–996.
Verbist, K., Baetens, J., Cornelis, W.M., Gabriels, D., Torres, C., Soto, G., 2009. Hydraulic conductivity as influenced by stoniness in degraded drylands of Chile. Soil Sci. Soc. Am. J. 73, 471–484.
Verbist, K.M.J., Cornelis, W.M., Torfs, S., Gabriels, D., 2013. Comparing methods to determine hydraulic conductivities on stony soils. Soil Sci. Soc. Am. J. 77, 25–42.
Zhou, B., Shao, M., Shao, H., 2009. Effects of rock fragments on water movement and solute transport in a loess plateau soil. C.R. Geoscience 341, 462–472.